

Organic and mineral matter changes due to oil generation, saturation and expulsion processes based on artificial maturation experiments

I.V.A.F. SOUZA¹ C.V. ARAÚJO¹ T.R., MENEZES¹ L.F.C. COUTINHO¹ R. BINNOTTO¹ A.L.D. SPIGOLON¹ R.A. FONTES¹
E.V. SANTOS NETO¹ N.D.V.F. RONDON² J.G. MENDOÇA FILHO²

¹PETROBRAS, CENPES

Av. Horácio Macedo 950, Cidade Universitária, Ilha do Fundão, CEP: 21941-915, Rio de Janeiro, Brazil.
Souza e-mail: igorviegas@petrobras.com.br

²Instituto de Geociências, Universidade Federal do Rio de Janeiro

Av. Athos da Silveira 274, Ilha do Fundão, CEP 21.949-900, Rio de Janeiro, Brazil.

ABSTRACT

Hydrous pyrolysis experiments were conducted on immature organic-rich rock with type-I kerogen to evaluate petroleum generation, saturation and expulsion processes. The experiments were carried out under isothermal conditions at ten different temperatures (280° through 360°C) for nine different time spans between 18 and 144h. Rock samples recovered from the experiments were analyzed for total organic carbon (TOC–weight%), Rock-Eval pyrolysis, vitrinite reflectance (Ro%), spectral fluorescence and visual characterization of organic matter under the microscopy. TOC, S₂ and HI tend to decrease with increasing temperature and duration of the experiments as expected. The Ro% values reach up to 1.14% in the most severe experiment (*i.e.* 360°C/96h). The Ro% is believed to be suppressed due to hydrogen incorporation from bitumen. The bitumen production was observed with the increase of transformation index (TI) and two types of bitumen were differentiated by fluorescence color. The bitumen with yellow fluorescence was mainly composed of saturate and aromatic hydrocarbons that were probably generated earlier than the bitumen with brown fluorescence which is rich in NSO compounds. The greatest bitumen saturation occurs at TI around of 41% to 45%, when the S₁ reaches its highest values. The decrease of bitumen saturation and consequent oil expulsion is marked by a reduction in S₁ values and fluorescence color. This phenomenon occurs simultaneously with the development of fractures and voids in the mineral matrix which reduces the oil retention capability and facilitates the expulsion process. These observations enhanced the understanding of oil generation and saturation processes, as well as primary migration, expulsion and type of generated bitumen.

KEYWORDS | Hydrous pyrolysis. Oil generation. Primary migration. Suppressed-vitrinite. Organic petrography. Oil expulsion.

INTRODUCTION

Understanding the generation, saturation and expulsion processes of petroleum systems is very important for the estimation of the amount, distribution and composition of oils in petroleum exploration. This information is extremely important in order to reduce

the exploratory risk. However, there are three types of pyrolysis methods (hydrous pyrolysis, closed anhydrous pyrolysis and open anhydrous pyrolysis) that sometimes provide different results on important parameters such as the timing of oil generation. Such differences impact directly the extrapolation of experimental results when applied to geological conditions. Lewan (1994) discussed

the differences between the three pyrolysis methods and concluded that hydrous pyrolysis experiments are the laboratory methods closest to natural processes for understanding expulsion of oil in nature.

Hydrous pyrolysis experiments involve heating a rock or kerogen sample in liquid water at subcritical temperatures in a closed reactor (Lewan *et al.*, 1979; Lewan, 1985). Generated and expelled oils derived from hydrous pyrolysis experiments are compositionally similar to natural crude oils and are typically a free-flowing liquid oil (Winters *et al.*, 1983). Although the processes responsible for the expulsion of oil are conceivably the same as those in nature (Lewan, 1991), the amount of expelled oil may be exaggerated as discussed by Lewan *et al.* (1995).

The main objective of this study is the observation of modifications on the organic matter and rock matrix during the oil generation and expulsion processes.

SAMPLE AND GEOLOGICAL INFORMATION

The Tremembé Formation sample from Taubaté Basin, Brazil, was selected for the hydrous pyrolysis experiments because it is a type I kerogen with high hydrocarbon source rock potential that can be used as an analogue for Brazilian source rock in order to assess the generation, expulsion and migration processes.

The Taubaté Basin located in the northeast of São Paulo State is 170km long in a NNW–SSE direction and about 20km wide, with an average sedimentary thickness of 800m (Fernandes, 1993). It is part of a taphrogenic set of basins belonging to the Southeastern Brazilian Continental Rift (RCSB), the origin of which is related to Tertiary distensive tectonic activity. The sediments are typically continental, with coarse granulometric sedimentary deposits at the basin fault edges, in addition to sandy and clay deposits in its central part, linked to fluvial–lacustrine sedimentation (Riccomini, 1989).

The Tremembé Formation, which belongs to the Oligocene-age Taubaté Group, is predominantly comprised of a sedimentary rock succession composed of siltstones, mudstones and shales rich in organic matter that represents a closed lacustrine, oligomitic, and eutrophic system developed in a semiarid climate (Ribeiro, 2004). Fernandes (1993) described the Tremembé Formation as being composed of compacted mudstones, papyraceous shales, rhythmites (marl/limestone intercalation and shale), sandstones, and limestones. These deposits of the Tremembé Formation have an irregular tabular geometry, with a known maximum thickness of about 400m.

METHODS

Hydrous Pyrolysis

Hydrous pyrolysis is a closed-system method of thermally decomposing organic matter in the presence of liquid water (Lewan *et al.*, 1979). One-liter stainless-steel reactors were filled with 275g gravel-sized (0.5–2cm) pieces of selected sample which are loaded into a one-liter Hasteloy-c reactor with enough distilled water to insure that the rock is submerged in liquid H₂O at subcritical experimental temperatures (lower than 374°C) before, during and after the experiments.

Specifics on the experimental protocol, collection procedure, reaction mechanisms, and character of the expelled oils are given in Lewan (1993, 1997). The temperatures are monitored within a standard error less than $\pm 0.5^\circ\text{C}$ with calibrated J-type thermocouples. Hydrous pyrolysis experiments were conducted in the USGS laboratory on immature organic-rich rock of the Tremembé Formation (Table I.1). The experiments were carried out under isothermal conditions at ten different temperatures (280°C through 360°C) and nine different time spans between 18 and 144h. The oil, gas and residual rock were collected and measured from each experiment for mass balance and geochemical analyses.

Total Organic Carbon (TOC) and Rock-Eval pyrolysis

An aliquot of the original sample from the Tremembé Formation and aliquots of the residual rocks recovered from hydrous pyrolysis experiments were pulverized and sieved in an 80 mesh granulometry for the analyses of total organic carbon (TOC-weight%) and Rock-Eval pyrolysis.

Inorganic carbon was removed with hydrochloric acid. TOC contents were determined by combustion in a Leco SC-144 carbon analyzer with an infrared detector. The insoluble residue (IR-%) was calculated using insoluble weight divided by sample weight multiplied by 100. The sample with TOC higher than 0.4% was analyzed for Rock-Eval pyrolysis. Free hydrocarbon (S₁), hydrocarbon source-rock potential (S₂), CO₂ organic source (S₃), maximum temperature at S₂ peak (T_{max}) and hydrogen and oxygen indices (HI and OI) were determined with a Rock-Eval 6 instrument (Behar *et al.*, 2001).

Sample preparation analyses

For maturation and type of organic matter studies it is necessary to isolate the kerogen. The standard non-oxidative palynological procedures for kerogen isolation utilized were described by Tyson (1995) with the modifications proposed by Oliveira *et al.* (2004). For kerogen concentrate preparation, the studied samples

were ground to approximately 2mm size. Samples were treated successively to remove carbonates (HCl 37% for 18h), silicates (HF 40% for 24h), and neoformed fluorides (HCl 37% for 3h). Between steps, samples were washed with distilled water until neutral. After this procedure, ZnCl₂ (density=1.9 to 2g/cm³) was added, stirred, and then centrifuged in order to separate sulphides. The floated material was washed similarly and HCl (10%) drops+distilled water were added to eliminate the heavy liquid. The isolated kerogen was sieved to 20µm. After this procedure, strew slides were made with the organic residue.

Palynofacies

The palynofacies analyses involved the quantitative (counting from 300 to 500 particles) and qualitative (organic particle component identification) examination of the kerogen component groups and subgroups. The palynofacies analysis was carried out only in the original sample from the Tremembé Formation. These were achieved by means of microscopy techniques under transmitted white light and fluorescence mode. The count followed the organic matter groups and subgroups classification proposed by Tyson (1995), Mendonça Filho (1999) and Menezes *et al.*, (2008). Following the organic particulate component count, absolute values were recalculated for percentages and normalized to 100%.

Maduration analyses

Spore coloration index (SCI), fluorescence analyses (%Ro) and vitrinite reflectance were carried out in order to access the maturation stage. The SCI used in this study was proposed and described by Barnard *et al.* (1981). It is a scale of 1 to 10 with intervals of 0.5 comprising 19 individual slides. The color of the sporomorphs increases with the increment of maturation due to increasing depth and temperature. Spectral fluorescence measurements were carried out with a Zeiss Axioskop 2-plus microscope, with 50X magnification in immersion oil ($n_c=1.518$ to 23°C), and (Zeiss) ultraviolet G 365, FT 395 and LP 420 filters coupled with a spectrometer J&M. The correction factor was obtained based on a calibrated lamp source (Baranger *et al.*, 1991). Spectral fluorescence analyses were performed on selected *Botryococcus* colonies using calibration procedures described by Araujo *et al.* (2002) and Araujo *et al.* (2003).

Mean random vitrinite reflectance measurements (Ro%) were carried out on whole rock polished sections using a Zeiss Axioskop 2-plus; 50X oil immersion objective, Zeiss immersion oil ($n_c = 1.518$; 23°C). Standards with known reflectance used were Klein & Beckers.

Visual Rock Characterization

The observation of whole rock plugs derived from the original sample and hydrous pyrolyzed samples allowed the observation of matrix modifications (*i.e.* fractures and holes) and bitumen impregnation. These observations associated to geochemical analyses brought insights in understanding the generation, saturation and oil expulsion processes.

There is a wide discussion in the literature on the definition of bitumen and there are a lot of similar terms as pyrobitumen, solid bitumen, migrabitumen, reservoir bitumen, dead oil, and exudatinitite (Abraham, 1960; Tissot and Welte, 1984; Curiale, 1986; Jacob, 1989; Hunt, 1996; Taylor *et al.*, 1998). There are two main lines related to this subject: chemical and petrographic. The general chemical definition of bitumen is all the organic matter present in sedimentary rocks that is extractable with organic solvents (Tissot and Welte, 1984; Hunt, 1996). However, Vandenbroucke and Largeau (2007) highlight that the amount of extractable hydrocarbon will depend on the polarity of organic solvent. So, the real quantification of bitumen is problematic. Jacob (1989) presented a petrographic definition of bitumen (migrabitumen) as a secondary maceral, amorphous with its shape adapted to the form of the cavities that are being filled. The last one is the subject of this study.

RESULTS AND DISCUSSIONS

Quantitative Yields

The oil, water, rock and gas were recovered from each hydrous pyrolysis experiment (Table I.1). It was not possible to quantify bitumen because the extractions from recovered rocks did not show repeatability. The amount of oil and gas increases with the severity of experiments. Hydrocarbon gases are a small part of total gases. It is worth to mention that it was observed expelled oil at the initial organic matter transformation stage.

TOC and Rock-Eval Pyrolysis

The TOC and Rock-Eval pyrolysis results are presented in Table I.2. TOC, S₂ and HI tend to decrease with the increment of temperature and duration of the experiments as a function of petroleum generation and expulsion (Figs. 1 and 2). The TOC content is high, declining from 10.13% to 4.28%. The insoluble residue values do not show significant variation with the rise in duration and temperature of the experiments (Table I.2). The S₂ values are good to very good, ranging from 73.94 and 7.1mg HC/g rock.

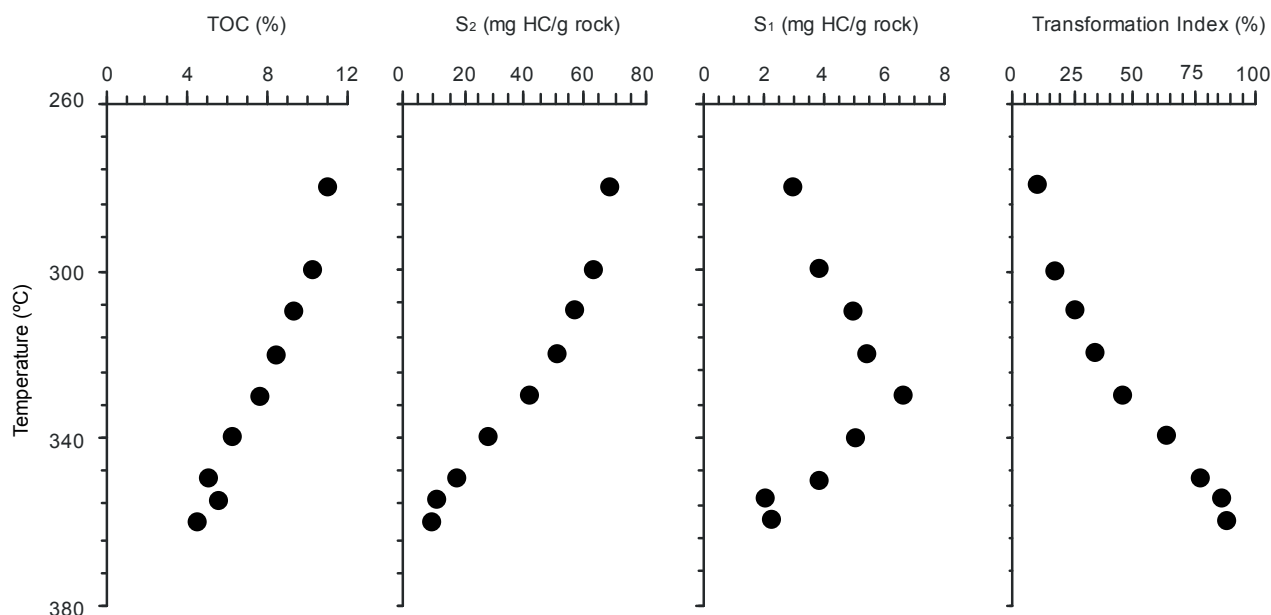


FIGURE 1. Variation of total organic carbon (TOC), free hydrocarbon (S_1), hydrocarbon source-rock potential (S_2) and transformation index (TI) with increasing experimental temperature for 72h.

The determination of level of kerogen cracking was based on the transformation index (TI) derived from Rock-Eval pyrolysis data (Tissot and Welte, 1984; Espitalié *et al.*, 1985 and Gonçalves *et al.*, 1997). The equation used was $(S_2(\text{Original}) - S_2(\text{Residual})) / S_2(\text{Original})$. The original S_2 utilized was the sum of S_1 and S_2 of the original sample from the Tremembé Formation. The Figure 3 shows the variation of TOC, S_1 , HI and T_{max} with the increase of TI.

The HI and OI plotted in a Van Krevelen type diagram (Espitalié *et al.*, 1987) show that the kerogen present in the Tremembé sample is type I. It is possible to observe trends in the Van Krevelen type diagram and in Langford and Blanc-Valleron graph related to the increase of transformation rates a function of thermal maturation (Figs. 4 and 5). The HI decreases from 730 to 166mg HC/g TOC. The OI of the original sample is very low and remains almost invariable with the increment of TI.

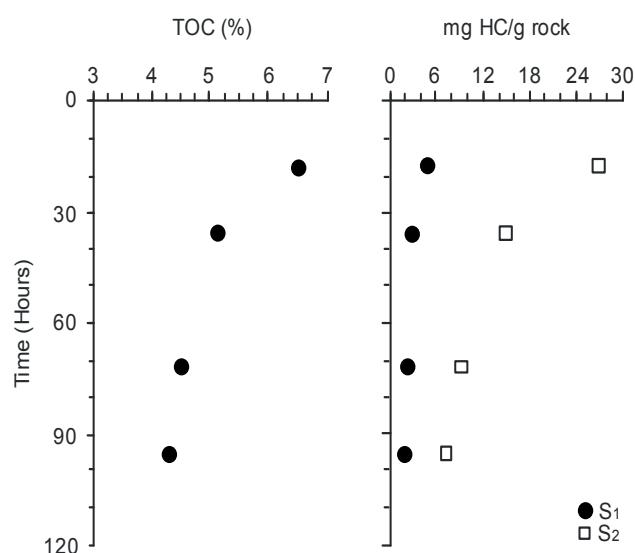


FIGURE 2. Variation of total organic carbon (TOC), free hydrocarbon (S_1) and hydrocarbon source-rock potential S_2 with the increment of experimental duration for 360°C isotherm.

The S_1 values reach up to 7.92mg HC/g rock around 41% to 45% of TI that was interpreted as a result of bitumen generation associated to the impregnation phase (Fig. 3). It is worth to mentioning that hydrocarbon expulsion associated with this phase was observed. After that, the S_1 values tend to decrease up to 1.75mg HC/g rock until the most severe experiment. The decrease of S_1 values was interpreted as an expulsion phase and shows good correlation with the increment of expelled oil. It is important to highlight that Alpern *et al.* (1993) pointed out that the S_1 yield does not correspond to the total free hydrocarbons in rocks, but only to the volatile fraction.

The T_{max} values present a similar behavior to the S_1 parameter and the highest value observed is 444°C that occurs around 41% to 45% of TI (Fig. 3). The decrease of T_{max} values with increasing TI can not be explained based on observed data. Theoretically, the S_2 values higher than 2mg HC/g rock would produce T_{max} values reliable for maturation assessment (Behar *et al.*, 2001). This behavior was previously discussed in the literature for the same type of kerogen by Espitalié (1986) and Bordenave (1993).

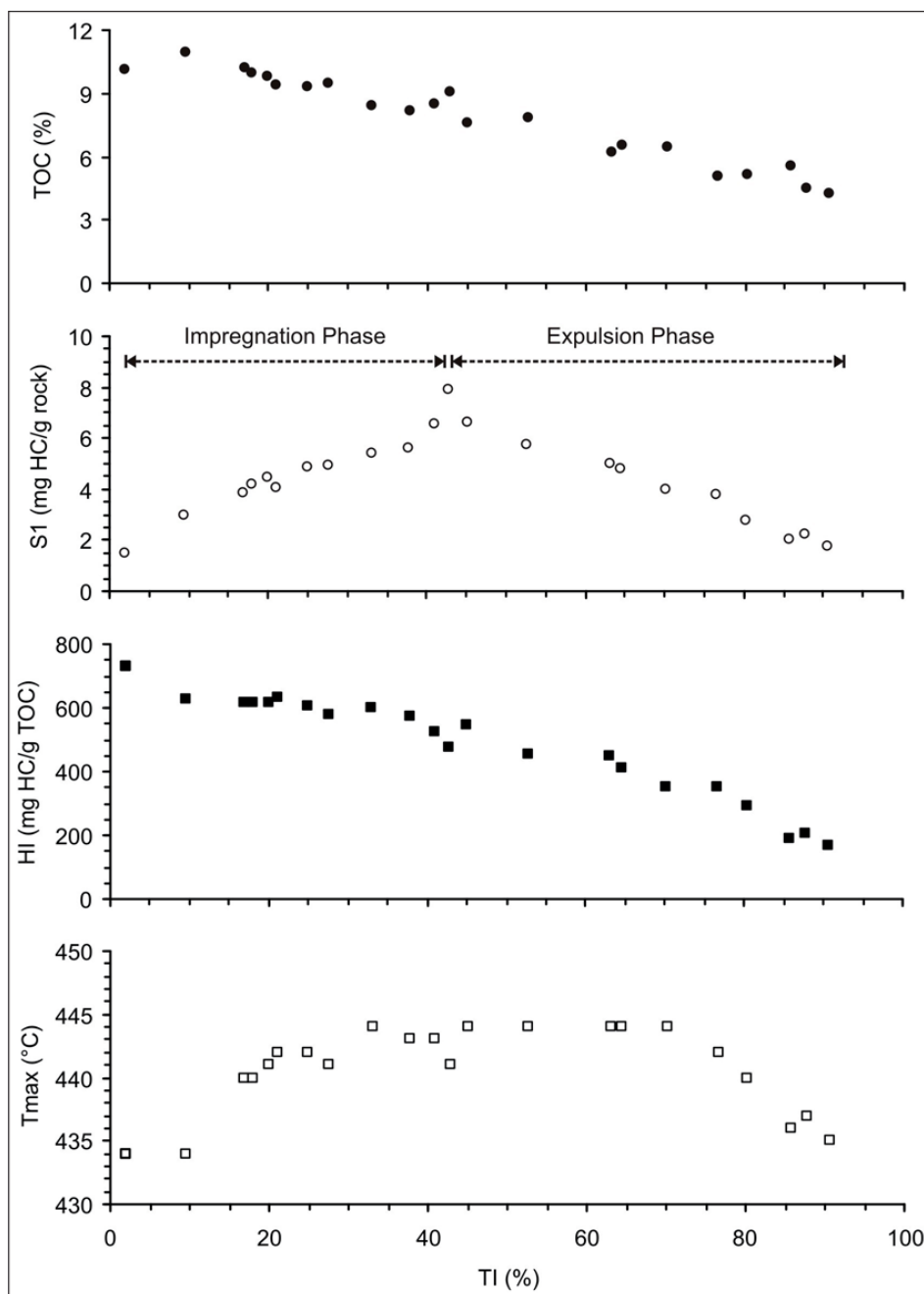


FIGURE 3. Variation of total organic carbon (TOC), free hydrocarbon (S_1), HI and T_{max} with the increment of transformation index (TI).

These authors suggested that T_{max} is not a good thermal maturation index for type I kerogen.

Palynofacies

The palynofacies analysis was carried out only in the original sample from the Tremembé Formation.

The palynofacies is characterized by a predominance of amorphous organic matter (AOM) with yellow fluorescence color (Table I.3 and Fig. 6). The Palynomorph group occurs with 15.5% and it is mainly represented by fresh water algae (*Botryococcus*) and sporomorphs (spores and pollen grains). Palynomorphs fluorescence color is yellow. The phytoclast group is the less abundant (1.6%)

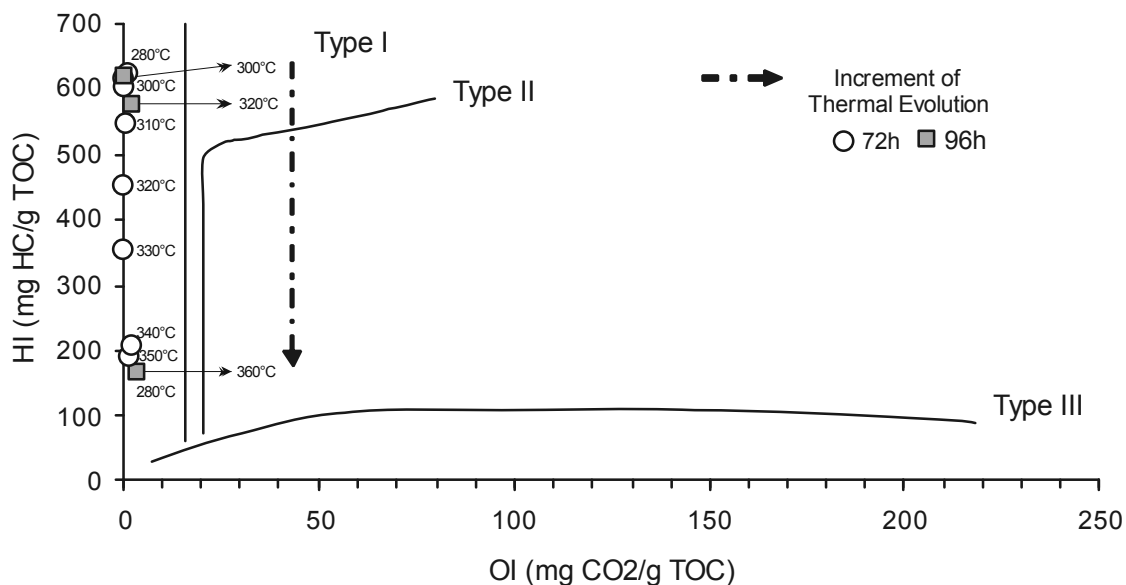


FIGURE 4. Van Krevelen type diagram for the original and pyrolyzed samples.

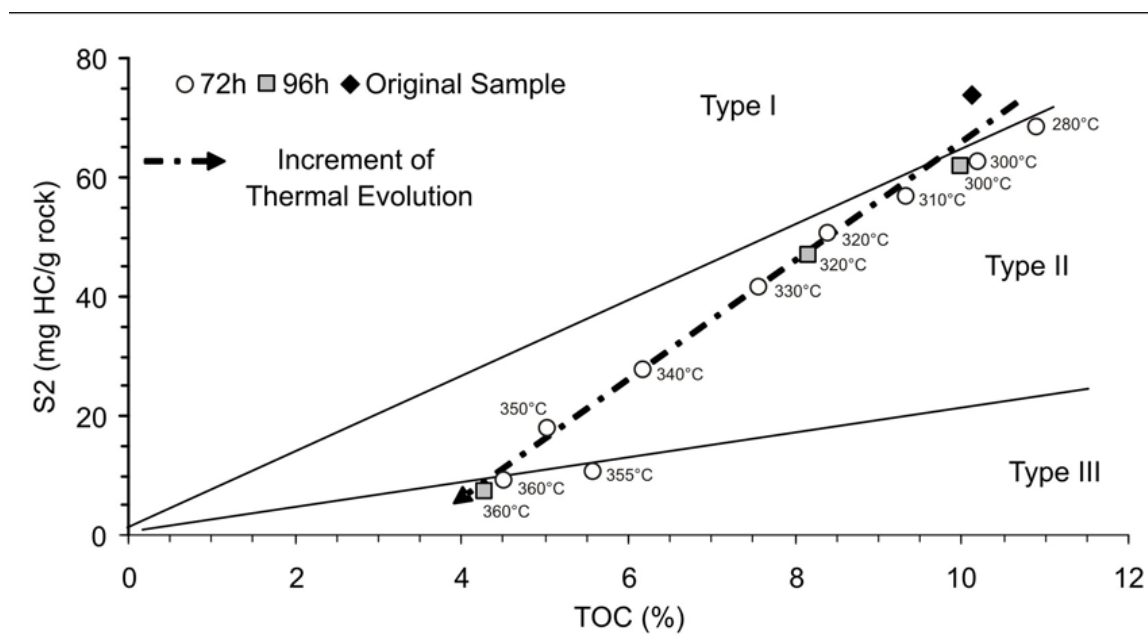


FIGURE 5. Classification of kerogen type based on hydrocarbon source-rock potential (S_2) and total organic carbon (TOC) data for the original and pyrolyzed samples (Langford and Blanc-Valleron, 1990).

and it is mainly represented by a biostructured non-opaque sub-group.

The high relative abundance of AOM is characteristic of areas with high organic matter preservation with intense microbiological reworking due to reducing conditions, especially in areas of high primary productivity (Tyson, 1993, 1995). Low energy areas, distant from fluvial-deltaic activity, also have elevated percentages of AOM (Tyson, 1993)

The palynofacies results are in agreement with the geochemical data and previous authors that pointed out Type-I kerogen for Tremembé Formation. (Soldan *et al.*, 1988; Mendonça Filho *et al.*, 2010).

Maturation

The evaluation of thermal evolution was based on the correlation of three optical parameters (Ro%, SCI and spectral fluorescence analysis). The maturation data is summarized in Table I.4.

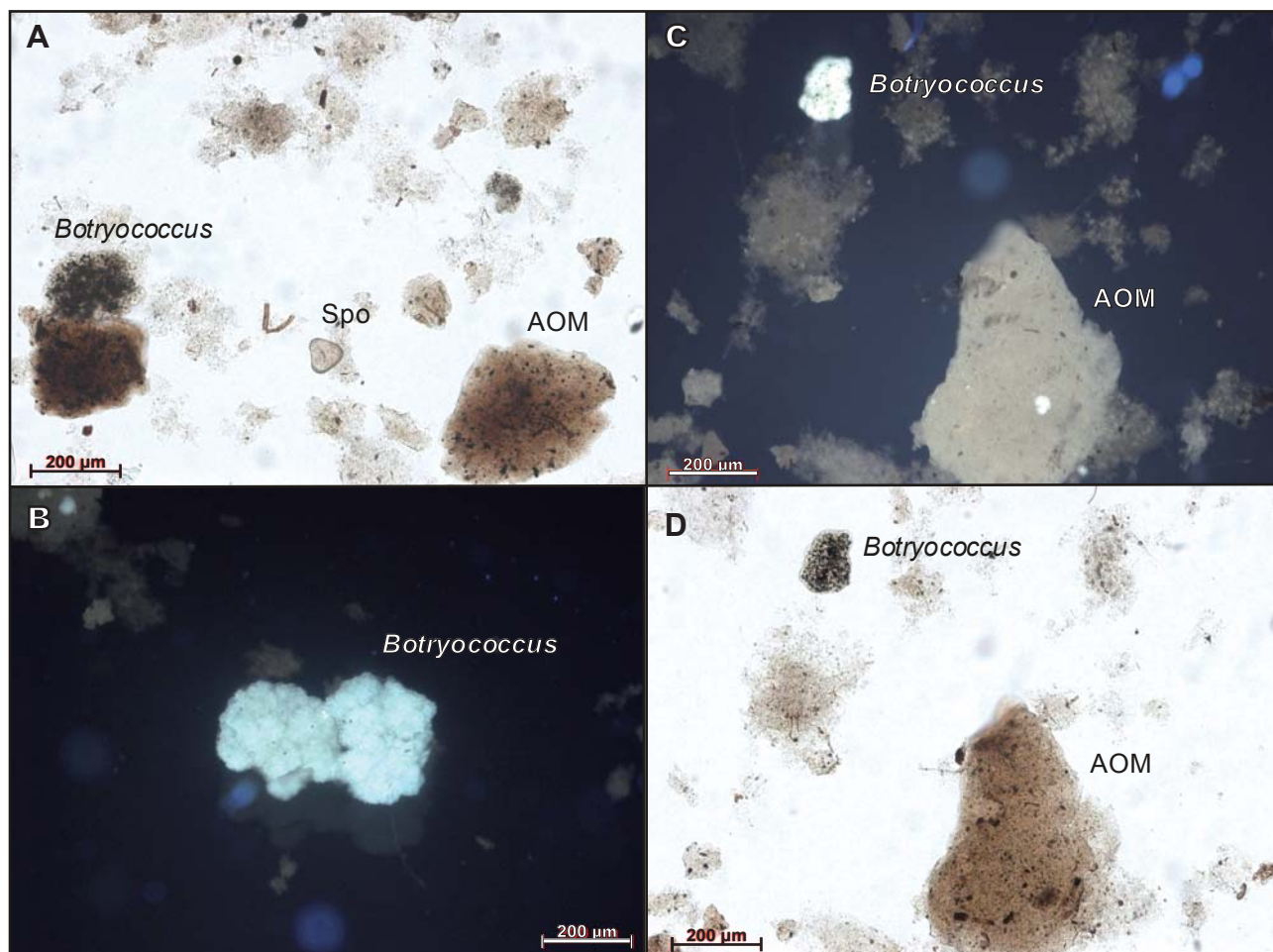


FIGURE 6. Photomicrographs of organic matter of the original sample. A) and D) transmitted light; B) and C) fluorescence mode.

The $Ro\%$ for the original sample is 0.32% which suggests a low stage of thermal evolution. SCI is 2.5 and can be correlated to Ro around 0.33%, showing a good correlation with $Ro\%$ data (Barnard *et al.*, 1981). Additionally, the λ_{max} derived from the corrected spectral curve of the original sample is 510nm that can be correlated to an $Ro\%$ around 0.33% (Mukhopadhyay, 1994). The $Ro\%$, SCI, spectral fluorescence and T_{max} results of the original sample presented good correlation and point out a low stage of thermal evolution. These results indicate that there is no evidence of suppression of vitrinite reflectance in the original sample.

The $Ro\%$ of the pyrolyzed samples ranges from 0.36% to 1.14%. The vitrinite reflectance values were plotted in the graph proposed by Bucharadt and Lewan (1990) that reveals the presence of suppressed-vitrinite phenomena (Fig. 7). Figure 8 shows the Ro with the increment of TI. It is possible to observe low Ro values associated to high TI which suggests

vitrinite suppression. There are a lot of mechanisms of suppression of vitrinite reflectance that were discussed by many authors (Hutton and Cook, 1980; Kalkreuth, 1982; Price and Barker, 1985; Bucharadt and Lewan, 1990; Mukhopadhyay, 1994; Suarez-Ruiz *et al.*, 1994; Carr, 2000). These results point out that the suppression of vitrinite reflectance occurred during the diagenesis of the organic matter and is most likely related to the saturation of vitrinite particles with bitumen or/and its association with hydrogen rich organic matter (liptinite). The suppression of vitrinite reflectance by impregnation of bitumen was reported before by Kalkreuth (1982), Suarez-Ruiz *et al.* (1994), Carr (2000) and Cuesta *et al.* (2005). Nevertheless, Barker *et al.* (2007) concluded that the suppression of vitrinite reflectance caused by bitumen impregnation is a rare phenomenon, but it may occur in huminite macerals (at low maturity stages). These authors analyzed samples with and without extraction and observed that the $Ro\%$ did not show significant changes. However, the impregnation by

bitumen can promote the incorporation of hydrogen in to the structure of vitrinite such that a simple extraction with organic solvent can not remove this effect.

Additionally, spectral fluorescence measurements were carried out on alginites (*Botryococcus*). The λ_{\max} derived from spectral fluorescence analyses reach up to 550nm at 9.54% of TI. After that, the λ_{\max} tends to decrease with increasing TI. This phenomenon was interpreted to be a result of bitumen influence. Spectral fluorescence made on the bitumen population with yellow fluorescence were carried out in each sample and do not show difference (λ_{\max} = 510nm). Figure 9 shows the spectral fluorescence curve measured on the bitumen observed in the polished sections and it is possible to notice the increment of the bitumen influence on the measured spectral curves. So, spectral fluorescence results of samples with TI higher than 9.54% were not considered reliable due to the bitumen influence.

Visual Rock Characterization

It was possible to observe morphologic changes on the organic matter and mineral matrix due to generation, saturation and expulsion process. Fluorescence color and abundance of *Botryococcus*, types of bitumen filling or impregnation, fluorescence of matrix (organic matter + bitumen impregnation) and development of holes and microfractures

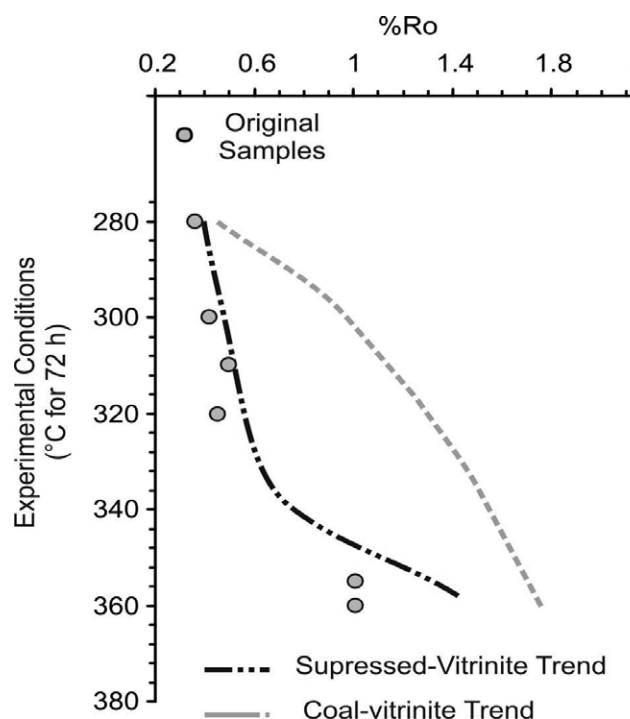


FIGURE 7. Variation of vitrinite reflectance Ro% with the rise of experimental temperature for 72 hours experiments (based on Buchardt and Lewan, 1990).

were observed in all samples. All the petrographic observation data is summarized in Table I.5.

Fluorescence Color and Relative Abundance of *Botryococcus* Algae

It is possible to observe changes in the fluorescence color of *Botryococcus* algae with the increment of the TI (Fig. I.1). The fluorescence color changes from yellow to dark orange. It is worth to mentioning that the samples derived from hydrous pyrolysis experiments with highest TI do not show fluorescence. Fluorescence intensity is related to the type, maturation and preservation of organic matter (Tyson, 1995, 2006). In this case, the reduction of fluorescence intensity can be attributed to the increment of thermal evolution. Additionally, the relative abundance of the *Botryococcus* algae tends to decrease with increasing of TI. This effect is interpreted to be a result of chemical composition of the *Botryococcus* algae that is extremely labile (Behar *et al.*, 1995). Development of holes exhibiting external borders with the same contour shape of *Botryococcus* bodies in the mineral matrix is interpreted as a result of *Botryococcus* decay with increasing severity of experimental conditions.

Relative Amount and Color of Bitumen Observed in Fluorescence Mode

The estimation of bitumen abundance was based on visual evaluation (Table I.5). The bitumen abundance increases until TI around 41 and 45%. Additionally, two types of bitumen were differentiated by fluorescence color (yellow and brown). Jacob (1989) proposed a classification of bitumens based on the physical and chemical properties and classified the bitumen with yellow fluorescence as ozocerite and with brown fluorescence as grahamite. Ozocerite bitumen is mainly composed by saturate fraction, more than 58% (Jacob, 1989). On the other hand, grahamite tends to present low content of saturated and aromatic hydrocarbons (lower than 3% and 13%, respectively). Fluorescence is produced by particular compounds ("fluorophor" or "chromophors") that exhibit specific type of carbon bonds (Robert, 1988, Lin and Davis, 1988). These authors observed that the fluorescence was enhanced when the fluorophors were dispersed throughout an aliphatic compound. In this study, the bitumen with yellow fluorescence (ozocerite) was probably generated before the bitumen with brown fluorescence (Fig. I.2 and Table I.5). These optical observations, that allowed us to interpret the chemical composition of bitumens, suggest that: i) composition of this specific organic matter from the Tremembé Formation (type-I kerogen - AOM and *Botryococcus*) favored the generation of the saturated and aromatic compounds in the low stages of the thermal evolution; ii) the first expelled oils are probably

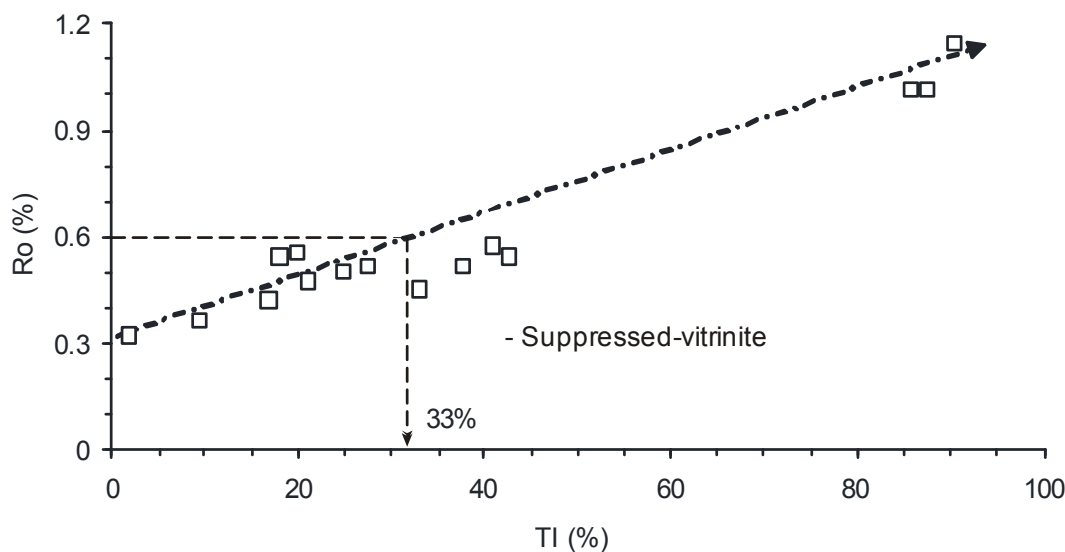


FIGURE 8. Variation of vitrinite reflectance Ro% with the increase of transformation index (TI).

rich in saturate and aromatic compounds, probably due to the mobility of these compounds. The migration of NSO compounds within the source rock is probably hampered by their size and chemical structure complexity. Unfortunately, it was not possible to present reliable SARA data from the oils to confirm this hypothesis, due to the high loss in the gravimetric column. Data on these experiments will be object of a future publication. However, Spigolon *et al.* (2013) carried out hydrous pyrolysis experiments on type-I kerogen from Lower Cretaceous Brazilian source rock, that presents similar organic matter composition than the sample from the Tremembé Formation. These authors carried out SARA and API gravity analysis of oils and observed an inverse trend with API decreasing with increasing temperature at 72h time span, which corroborates the proposed hypothesis of this paper. Spigolon *et al.* (2013) suggested that this unexpected behavior is related to the polar compounds that remain trapped in the source rock. Nevertheless, it is possible to observe, through microscope examination, that the first generated bitumen was ozocerite and the composition of the first expelled oil should be similar to this type of bitumen. This interpretation does not agree with data in the literature (Tissot and Welte, 1984; Lewan, 1983; Hunt, 1996), which show that bitumen are rich in NSO compounds, but our data suggest an unexpected behavior that could be related to this specific organic matter rich in lipid compounds. It is worth to mention that the increment of bitumen presents good correlation with S_1 values from pyrolysis Rock-Eval. As mentioned before, Alpern *et al.* (1993) pointed out that the S_1 yield does not correspond to the total free hydrocarbons in rocks. However, this good correlation can be attributed to the predominance of bitumen with yellow fluorescence (ozocerite) until TI around 45%.

Matrix Fluorescence

The bitumen impregnation of the mineral matrix was detected because of the increasing fluorescence of the mineral matrix (Fig. I.3). The main bitumen impregnation stage occurs with a TI around 41% to 45%, when the S_1 reaches its highest values. The decrease in bitumen impregnation is marked by a reduction in S_1 values and fluorescence color consequence of an important phase of oil expulsion. It was very interesting to notice that there are levels with high fluorescence which point out some preferential routes of bitumen migration within the source rock (Fig. I.4). This phenomenon is attributed to the different permeabilities and trends to follow the rock lamination.

Abundance of Microfractures

It was noticed a positive correlation between the TI and the number of fractures and holes (Fig. I.5). Talukdar *et al.* (1986) carried out petrographic studies of thin sections and polished slabs of La Luna Formation, which is the major source rock of the Maracaibo Basin, Venezuela. These authors believe that the oil generation opened pre-existing fractures and created new ones as a consequence of an increase in the volume of the pore fluid resulting from the partial thermal transformation of kerogen to bitumen, oil and gas. It is interesting to notice that the fractures of the Tremembé samples with low TI tend to present a higher number of fractures following the lamination of the rock. However, the samples with high TI show fractures in all directions that facilitate the oil migration and expulsion. The rise in the number of fractures led to the reduction of the fluorescence color of the mineral matrix and the S_1 values. Lewan (1987) and Lewan and Roy (2011) attributed

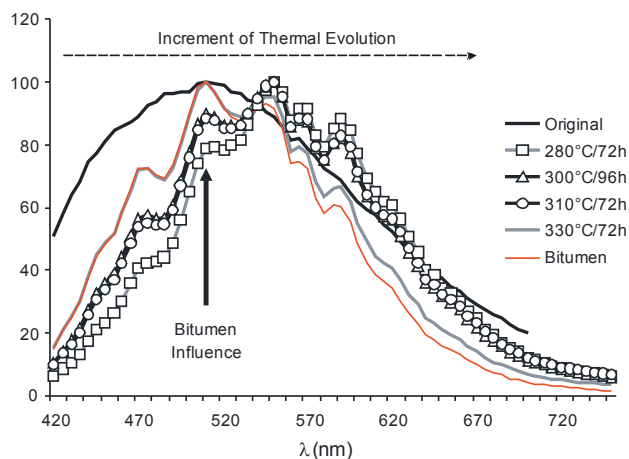


FIGURE 9. Spectral fluorescence of original, bitumen and pyrolyzed samples.

the fracture generation to tensile stress generated by the expansion associated with kerogen conversion to bitumen and bitumen conversion to oil.

CONCLUSIONS

The studied sample from the Tremembé Formation is immature. Both palynofacies and Rock-Eval pyrolysis analyses indicate a Type-I kerogen deposited in a lacustrine setting with low fluvial input.

The aliquots derived from hydrous pyrolysis experiments show an increase of thermal cracking and expelled products (oil and gas) according to the increase of severity of the experiments (temperature and time) that promotes the diminishing of TOC, S_2 and HI.

The correlation between the Ro% values and transformation index (TI) suggests that the vitrinite reflectance is suppressed. The results lead to believe that the suppression of vitrinite reflectance can be associated to hydrogen incorporation from increasing bitumen availability and organic facies (hydrogen rich organic matter).

The S_1 values reach up to 7.92mg HC/g rock around 41% to 45% of TI which was interpreted as a result of generation associated to mineral matrix impregnation processes. After that, the number of microfractures became significant and the S_1 values tend to decrease most likely due to the reduction of capability retention and bitumen cracking. Samples derived from the first set of experiments show microfractures that tend to occur parallel to the layer (lamination). On the other hand, fractures of samples with high TI are observed with various orientations.

The abundance of bitumen increases with TI and two types of bitumen were observed on microscopy analyses. The yellow fluorescence bitumen was probably generated earlier than brown fluorescence bitumen. Most likely, the yellow fluorescence bitumen (ozocerite) is rich in aliphatic and aromatic compounds. These observations lead us to interpret that the first generated oils are rich in aromatic and aliphatic compounds and this is directly linked to the type of organic matter and the facility of migration of these compounds.

The observation of bitumens, impregnation of the rock matrix by bitumen, microfractures and the fluorescence and abundance of *Botryococcus* algae brings insight to the understanding of generation, primary migration and expulsion processes of this specific organic matter (highly oil-prone lacustrine source rocks).

ACKNOWLEDGMENTS

The authors thank Petrobras for allowing the publication of this study and the USGS for technology transfer and laboratory support. We are grateful to Ángeles Borrego and Rolando di Primio for critical comments that improved the manuscript. We want to recognize and give a special thanks to Michael Lewan for his suggestions and support.

REFERENCES

- Abraham, H., 1960. Asphalts and Allied Substances. 1. Historical Review and Natural Raw Materials. Princeton, New Jersey, Princeton University Press, 370pp.
- Alpern, B., Lemos de Souza, M.J., Pinheiro, H.J., Zhu, X., 1993. Detection and evaluation of hydrocarbons in source rocks by fluorescence microscopy. *Organic Geochemistry*, 20(6), 789-795.
- Araujo, C.V., Kalkreuth, W., Stasiuk, L., Pickel, W., Newman, J., Condé, V.C., 2002. Interlaboratory studies on thermal indices of Torbanite samples from Australia. 8th Latin American Congress on Organic Geochemistry, Cartagena, Colombia (2002), 31-34.
- Araujo, C.V., Barbanti, S.M., Condé, V.C., Kalkreuth, W., Macedo, A.C., Newman, J., Pickel, W., Stasiuk, L., Volk, H., 2003. Thermal Indices Working Group: Summary of the 2002 Round Robin Exercise. *International Committee for Coal and Organic Petrology News*, 29, 5-12.
- Baranger, R., Martinez, L., Pittion, J.L., Pouleau J., 1991. A new calibration procedure for fluorescence measurements of sedimentary organic matter. *Organic Geochemistry*, 17 (4), 467-475.
- Barker, C.E., Lewan, M.D., Pawlewicz, M.J., 2007. The influence of extractable organic matter on vitrinite reflectance suppression: A survey of kerogen and coal types. *International Journal of Coal Geology*, 70 (1-3), 67-78.
- Barnard, P.C., Collins, A.G., Cooper, B.S., 1981. Generation of

- hydrocarbons – Time, temperature and source rock quality. In: Brooks, J. (ed.). *Organic Maturation Studies and Fossil Fuel Exploration*. London, Academic Press, 337-342.
- Behar, F., Derenne, S., Largeau, C. 1995. Closed pyrolyses of the isoprenoid algaenan of *Botryococcus braunii*, L race: geochemical implications for derived kerogens. *Geochimica et Cosmochimica Acta*, 59 (14), 2983-2997.
- Behar, F., Beaumont, V., Penteado, H.L. De B., 2001. Rock-Eval 6 technology: performances and developments. *Oil & Gas Science and Technology Revue IFP*, 56 (2), 111-134.
- Bordenave, M.L., 1993. *Applied Petroleum Geochemistry*. Paris, Editions Technip, 524pp.
- Buchardt, B., Lewan, M.D., 1990. Reflectance of vitrinite-like macerals as a thermal maturity index for Cambrian–Ordovician Alum Shale, southern Scandinavia. *American Association of Petroleum Geologists Bulletin.*, 74, 394-406.
- Carr, A.D., 2000. Suppression and retardation of vitrinite reflectance, Parts 1. *Journal of Petroleum Geology*, 23, 313-343.
- Cuesta, M.J., Rubiera, F., Arenillas, A., Iglesias, M.J., Suárez-Ruiz, I., Pis, J.J., 2005. Evaluation of the combustion behavior of perhydrous coals by thermal analysis. *Journal of Thermal Analysis and Calorimetry*, 81, 333-337.
- Curiale, J.A., 1986. Origin of solid bitumens, with emphasis on biological marker results. *Organic Geochemistry*, 10, 559-580.
- Espitalié, J., 1986. Use of Tmax as a maturation index for different types of organic matter. Comparison with vitrinite reflectance. *Thermal Modelling in Sedimentary Basins*, Technip, 475–496.
- Espitalié, J., Deroo, G., Marquis, F., 1985. La pyrolyse Rock-Eval et ses Applications - première/deuxième partie. *Revue de l'Institut Français du Pétrole*, 40 (5-6), 563-579.
- Espitalié, J., Marquis, F., Sage, L., 1987. Organic geochemistry of the Paris Basin. In: Brooks, J., Glennie, K.W. (eds.). *Petroleum Geology of North West Europe*. London, Graham&Trotman, 71-86.
- Fernandes, F.L., 1993. Arcabouço estrutural e evolução da bacia de Taubaté –SP. Masters Thesis, Ouro Preto Federal University. 147pp.
- Gonçalves, F.T.T., Araujo, C.V., Penteado, H.L.B., Hamsi Jr., G.P., Frota, E.S.T., Soldan, A.L., 1997. Séries Naturais: Aplicação no Estudo da Geração e Expulsão do Petróleo e no Mapeamento de Oil-Kitchens. *Boletim de Geociências da Petrobras*, 11 (1-2), 116-131.
- Hunt, J.M., 1996. *Petroleum Geochemistry and Geology*. 2nd ed. New York, W.H. Freeman and Company, 743pp.
- Hutton, A., Cook, A., 1980. Influence of alginite in the reflectance of vitrinite from Joadja, NSW and some other coals and oil shales containing alginite. *Fuel*, 59 (10), 711-716.
- Jacob, H., 1989. Classification, structure, genesis and practical importance of natural solid oil bitumen (“migrabitumen”). *International Journal of Coal Geology*, 11, 65-79.
- Kalkreuth, W.D., 1982. Rank and petrographic composition of selected Jurassic–Lower Cretaceous coals of British Columbia, Canada. *Bulletin of Canadian Petroleum Geology*, 30, 112–139.
- Lewan, M.D., 1985. Evaluation of petroleum generation by hydrous pyrolysis experimentation. *Philosophical Transactions of the Royal Society of London Series A*, 315, 123-134.
- Lewan, M.D., 1987. Petrographic study of primary petroleum migration in the Woodford Shale and related rock units. In: Doligez, B. (ed.). *Migration of Hydrocarbons in Sedimentary Basins*. Paris, Editions Technip, 113-130.
- Lewan, M.D., 1991. Primary oil migration and expulsion as determined by hydrous pyrolysis. *Proceedings of the 13th World Petroleum Congress*, 2, 215-223.
- Lewan, M.D., 1993. Laboratory simulation of petroleum formation-hydrous pyrolysis. In: Engel, M., Macko, S. (eds.). *Organic Geochemistry - Principles and Applications*. New York, Plenum Press, 419-442.
- Lewan, M.D., 1994. Assessing natural oil expulsion from source rocks by laboratory pyrolysis. In: Dow, W., Magoon, L., (eds.). *The Petroleum System-From Source to Trap*. American Association of Petroleum Geologists Memoir 60, 201-210.
- Lewan, M.D., 1997. Experiments on the role of water in petroleum formation. *Geochimica et Cosmochimica Acta*, 61, 3691-3723.
- Lewan, M.D., Roy, S., 2011. Role of water in hydrocarbon generation from Type-I kerogen in Mahogany oil shale of the Green River Formation. *Organic Geochemistry*, 42, 31-41.
- Lewan, M.D., Winters, J.C., McDonald J.H., 1979. Generation of oil-like pyrolyzates from organic-rich shales. *Science*, 203, 897-899.
- Lewan, M.D., Comer, J.B., Hamilton-Smith, T., Hausenmuller, N.R., Guthrie, J.M., Hatch, J.R., Gautier, D.L., Frankie, W.T., 1995. Feasibility study on material-balance assessment of petroleum from the New Albany Shale in the Illinois Basin. *United States Geological Survey Bulletin*, 2137, 31pp.
- Lin, R., Davis, A., 1988. The chemistry of coal maceral fluorescence: with special reference to the huminite/vitrinite group. Special Research Report, Energy and Fuel Research Center, Pennsylvania State University, SR-122, 278pp.
- Mendonça Filho, J.G., 1999. Aplicação de estudos de palinofácies e fácies orgânicas em rochas do Paleozóico Superior da Bacia do Paraná, sul do Brasil. Doctoral Thesis. Rio Grande do Sul Federal University, 254pp.
- Mendonça Filho, J.G., Chagas, R.B.A., Menezes, T.R., Mendonça, J.O., da Silva, F.S., Sabadini-Santos, E., 2010. Organic facies of the Oligocene lacustrine system in the Cenozoic Taubaté Basin, Southern Brazil. *International Journal of Coal Geology*, 84, 166-178.
- Mendonça Filho, J.G., Menezes, T.R., Mendonça, J.O., Oliveira, A.D., Carvalho, M.A., Sant Anna, A.J., Souza, J.T., 2010. Palinofácies. In: Souza, I.C. (ed.). *Paleontologia*. Interciência. Rio de Janeiro, 2, 379-413.
- Menezes, T.R., Mendonça Filho, J.G., Araújo, C.V., Souza, I.V.A.F., Mendonça, J.O., 2008. Fácies Orgânica: conceitos, métodos e estudos de casos na indústria do petróleo. *Revista Brasileira Geociências*, 38, 80-96.
- Mukhopadhyay, P.K., 1994. Vitrinite reflectance as maturity parameter. Petrographic and molecular characterization and its applications to basin modeling. In: Dow, W.G., Mukhopadhyay, P.K. (eds.). *Vitrinite Reflectance as*

- a Maturity Parameter. Applications and Limitations. Washington, America Chemical Society, 1-24.
- Oliveira, A.D., Mendonça Filho, J.G., Carvalho, M.A., Menezes, T.R., Lana, C.C., Brenner, W.W., 2004. Novo método de preparação palinológica para aumentar a recuperação de dinoflagelados. *Revista Brasileira de Paleontologia*, 7 (2), 169-175.
- Price, L.C., Barker, C.E., 1985. Suppression of vitrinite reflectance in amorphous rich kerogen a major unrecognized problem. *Journal of Petroleum Geology*, 8, 59-84.
- Ribeiro, M.T., 2004. Fácies microclásticas de um sistema lacustre oligocênico do Sudeste do Brasil (Formação Tremembé, bacia de Taubaté). Masters Thesis. Rio de Janeiro Federal University, 122pp.
- Riccomini, C., 1989. O rift continental do Sudeste do Brasil. Doctoral Thesis. São Paulo University, 256pp.
- Robert, P., 1988. Organic Metamorphism and geothermal history: Microscopic study of organic matter and thermal evolution of sedimentary basins. Reidel, Dordrecht, 311pp.
- Soldan, A.L., Santos Neto, E.V., Cerqueira, J.R., Concha, F.J.M., Branco, V.A.C., Arai, M., 1988. Hidropirólise: uma nova ferramenta para o estudo do processo de maturação. *Bol. de Geociências da Petrobrás*, 2 (1), 65-76.
- Spigolon, A.L.D., Lewan, M.D., Mendonça Filho, J.G., Penteadó, L.H.B., Coutinho, L.F.C., 2013. New insights on changes in the oil quality during petroleum formation by hydrous pyrolysis on a Brazilian source rock containing Type-I kerogen. Abstracts. Costa Adeje, Tenerife, Spain, 26th International Meeting on Organic Geochemistry 1, 417-418.
- Surez-Ruiz, I., Iglesias, M.J., Jimnez, A., Laggoun, D.F., Prado, J.G., 1994. Petrographic and geochemical anomalies detected in Spanish Jurassic jet. In: Dow, W.G., Mukhopadhyay, P.K. (eds.). *Vitrinite Reflectance as a Maturity Parameter. Applications and Limitations*. Washington, America Chemical Society, 76-92.
- Talukdar, S., Gallongo, O., Chin-A-Lien, M., 1986. Generation and Migration of hydrocarbons in the Maracaibo Basin, Venezuela: An Integrated basin study. *Organic Geochemistry*, 10, 261-279.
- Taylor, G.H., Teichmuller, M., Davis, A., Diessel, C.F.K., Littke, R., Robert, P., 1998. *Organic Petrology*. Berlin, Gebrüder Borntraeger, 704pp.
- Tissot, B.P., Welte, D.H., 1984. *Petroleum Formation and Occurrence*. 2 ed. Berlin, Springer-Verlag, 699pp.
- Tyson, R.V., 1993. Palynofacies analysis. In: Jenkins, D.J. (ed.). *Applied Micropaleontology*. Dordrecht, Kluwer Academic Publishers, 153-191.
- Tyson, R.V., 1995. *Sedimentary Organic Matter*. London, Chapman & Hall, 615pp.
- Tyson, R.V. 2006. Calibration of hydrogen indices with microscopy: A review, reanalysis and new results using the fluorescence scale. *Organic Geochemistry*, 37 (1), 45-63.
- Vandenbroucke, M., Largeau, C., 2007. Kerogen origin, evolution and structure. *Organic Geochemistry*, 38, 719-833.
- Winters, J.C., Williams, J.A., Lewan, M.D., 1983. A laboratory study of petroleum generation by hydrous pyrolysis. In: Bjoroy, M. (ed.). *Advances in Organic Geochemistry*. New York, John Wiley, 524-533.

**Manuscript received March 2014;
revision accepted October 2014;
published Online November 2014.**

ELECTRONIC APPENDIX

TABLE I.1. Mass balance of recovered products from hydrous-pyrolysis experiments with Tremembé Formation Additional information: Added water (380g), Initial rock (275g). The data suggested that the rock samples presented wetness, which is the reason for the high recovered water values.

Temperature (°C)	Time (hours)	Recovered Water (g)	Recovered Rock Sample (g)	Expelled Oil (g)	Generated Gas (g)	HC Gases (g)	Recovery (%)
20	0						
280	72	236.3	403.4	0.387	2.938	0.126	98.13
300	72	230.8	407.0	1.426	3.991	0.233	98.17
300	96	231.6	398.6	1.494	3.637	0.239	96.98
300	120	231.1	409.6	1.231	3.821	0.261	98.54
300	144	229.0	412.8	2.038	4.199	0.29	98.99
310	72	228.5	409.1	1.65	4.157	0.296	98.20
320	36	224.6	412.2	2.059	4.346	0.351	98.20
320	72	227.1	409.1	3.476	4.913	0.412	98.37
320	96	223.1	412.2	5.038	5.055	0.453	98.50
320	120	224.5	409.2	4.13	5.202	0.497	98.17
340	36	222.3	413.2	5.01	5.218	0.582	98.55
330	72	224.6	408.8	4.737	5.255	0.539	98.14
340	48	221.3	409.4	7.193	5.558	0.602	98.24
340	72	219.2	409.5	6.725	5.566	0.694	97.80
360	18	215.9	364.9	9.359	5.653	0.786	90.94
340	108	217.7	410.5	8.721	5.559	0.754	98.09
350	72	212.4	414.6	9.769	5.847	0.901	98.08
360	36	214.8	411.8	10.048	5.919	0.94	98.00
355	72	213.5	412.4	10.131	6.051	0.992	97.97
360	72	213.7	411.8	11.481	6.379	1.141	98.19
360	96	209.4	414.0	12.694	6.663	1.345	98.04

TABLE I.2. Total organic carbon (TOC) and Rock-Eval pyrolysis data and transformation index (TI) for the original sample and the residual rock

Temperature (°C)	Time (hours)	TOC (%)	IR	S1	S2	S3	HI	OI	Tmax	TI (%)
20	0	10.13	96	1.46	73.94	1.07	730	11	434	
280	72	10.90	88	2.95	68.21	0.13	626	1	434	9.54
300	72	10.20	92	3.82	62.59	0.00	614	0	440	16.99
300	96	10.00	92	4.19	61.82	0.00	618	0	440	18.01
300	120	9.81	92	4.47	60.31	0.13	615	1	441	20.01
300	144	9.41	96	4.04	59.49	0.29	632	3	442	21.10
310	72	9.33	92	4.89	56.56	0.00	606	0	442	24.99
320	36	9.48	92	4.91	54.61	0.11	576	1	441	27.57
320	72	8.39	92	5.41	50.51	0.00	602	0	444	33.01
320	96	8.16	96	5.60	46.92	0.17	575	2	443	37.77
320	120	8.52	84	6.56	44.52	0.28	523	3	443	40.95
340	36	9.08	92	7.92	43.10	0.00	475	0	441	42.84
330	72	7.56	88	6.61	41.41	0.07	548	1	444	45.08
340	48	7.84	92	5.72	35.66	0.16	455	2	444	52.71
340	72	6.19	92	5.02	27.80	0.00	449	0	444	63.13
360	18	6.52	88	4.80	26.75	0.09	410	1	444	64.52
340	108	6.44	88	3.97	22.48	0.09	349	1	444	70.19
350	72	5.03	92	3.79	17.65	0.01	351	0	442	76.59
360	36	5.12	88	2.77	14.83	0.11	290	2	440	80.33
355	72	5.59	88	2.04	10.70	0.09	192	2	436	85.81
360	72	4.51	92	2.22	9.27	0.09	206	2	437	87.71
360	96	4.28	88	1.75	7.10	0.14	166	3	435	90.58

Units: TOC (Total Organic Carbon - wt%); IR (Insoluble residue - %); S1 (free hydrocarbon - mg HC/g rock); S2 (hydrocarbon source rock potential - mg HC/g rock); S3 (CO₂ - mg CO₂/g rock); HI (Hydrogen Index - mg HC/g, TOC); OI (Oxygen Index - mg CO₂/g TOC); TI (transformation index); Tmax (maximum temperature at S₂ peak - °C).

TABLE I.3. Palynofacies result of the original sample

AOM	Opaque	Bio	PHY	Botry	Spo	PAL
82.9	0.3	1.3	1.6	14	1.5	15.5

Legend: AOM (Amorphous Organic Matter -%); Opaque (Opaque Phytoclasts -%); Bio (Biostructured Phytoclasts -%); PHY (Phytoclasts -%); Botry (Botryococcus -%); Spo (Sporomorphs -%); PAL (Palynomorphs -%).
PHY=Opaque+Bio; PAL= Botry+Spo.

TABLE I.4. Vitrinite reflectance and fluorescence data

Time (Hours)	TI(%)	Ro(%)	N°M	SD	Spectral Fluoresc.	
					λ_{max}	Roeq.
0	1.94	0.32	5	0.04	510	0.33/0.35
72	9.54	0.36	9	0.09	550	0.55/0.42
72	16.99	0.42	6	0.06	550	0.55/0.38
96	18.01	0.54	9	0.08	550	0.55/0.36
120	20.01	0.55	4	0.08		
144	21.10	0.47	4	0.02		
72	24.99	0.5	2	0.11	550	0.55/0.38
30	27.57	0.51	1	-		
72	33.01	0.45	1	-	510	0.33/0.30
90	37.77	0.51	2	0.01		
120	40.95	0.57	2	0.04		
36	42.84	0.54	1	-		
72	45.08	-			510	0.33/0.28
100	52.71	-				
72	63.13					
36	64.52					
18	70.19					
72	76.59					
96	80.33					
72	85.81	1.01	8	0.05		
72	87.71	1.01	3	0.08		
96	90.58	1.14	5	0.04		

Legend: N°M (number of measurements); SD (standard deviation); λ_{max} (maximum fluorescence intensity); Q (red/green coefficient); Roeq (equivalent vitrinite reflectance based on the correlation chart proposed by Mukhopadhyay, 1994).

TABLE I.5. Petrographic observation data

Temperature (°C)	Duration (Hours)	TI(%)	Fluorescence			Matrix		
			Alginite	*Green Bitumen	*Brown Bitumen	Matrix (Impregnation)	*Vugs	*Fractures
20	0	1.94	GR	1	-	BR	-	1
280	72	9.54	YE	1	-	BR	-	1
300	72	16.99	YE	1	-	DOR	-	1
300	96	18.01	LOR	2	-	LOR	1	2
300	120	20.01	LOR	2	-	LOR	1	3
300	144	21.10	LOR	2	-	LOR	1	3
310	72	24.99	MOR	4	-	LOR	2	4
320	30	27.57	MOR	2	1	LOR	2	3
320	72	33.01	DOR	6	1	LOR	2	4
320	90	37.77	DOR	4	1	LOR	2	4
320	120	40.95	BR	5	1	YE	2	5
340	36	42.84	BR	7	3	YE	3	5
330	72	45.08	BR	7	4	YE	4	5
340	100	52.71	NF	7	3	YE	5	6
340	72	63.13	NF	7	5	LOR	5	6
360	36	64.52	NF	9	6	LOR	6	7
360	18	70.19	NF	9	5	LOR	8	7
350	72	76.59	NF	2	6	MOR	5	8
360	96	80.33	NF	7	6	MOR	5	8
355	72	85.81	NF	2	6	MOR	6	8
360	72	87.71	NF	2	6	MOR	6	8
360	96	90.58	NF	11	4	DOR	9	9

Legend: Fluorescence Color: GR (green); YE (yellow); LOR (light orange); MOR (middle orange); DOR (dark orange); BR (brown); NF (no fluorescence).

* Relative abundance scale built in order to give a comparative idea between the samples. Based on microscopic observation.

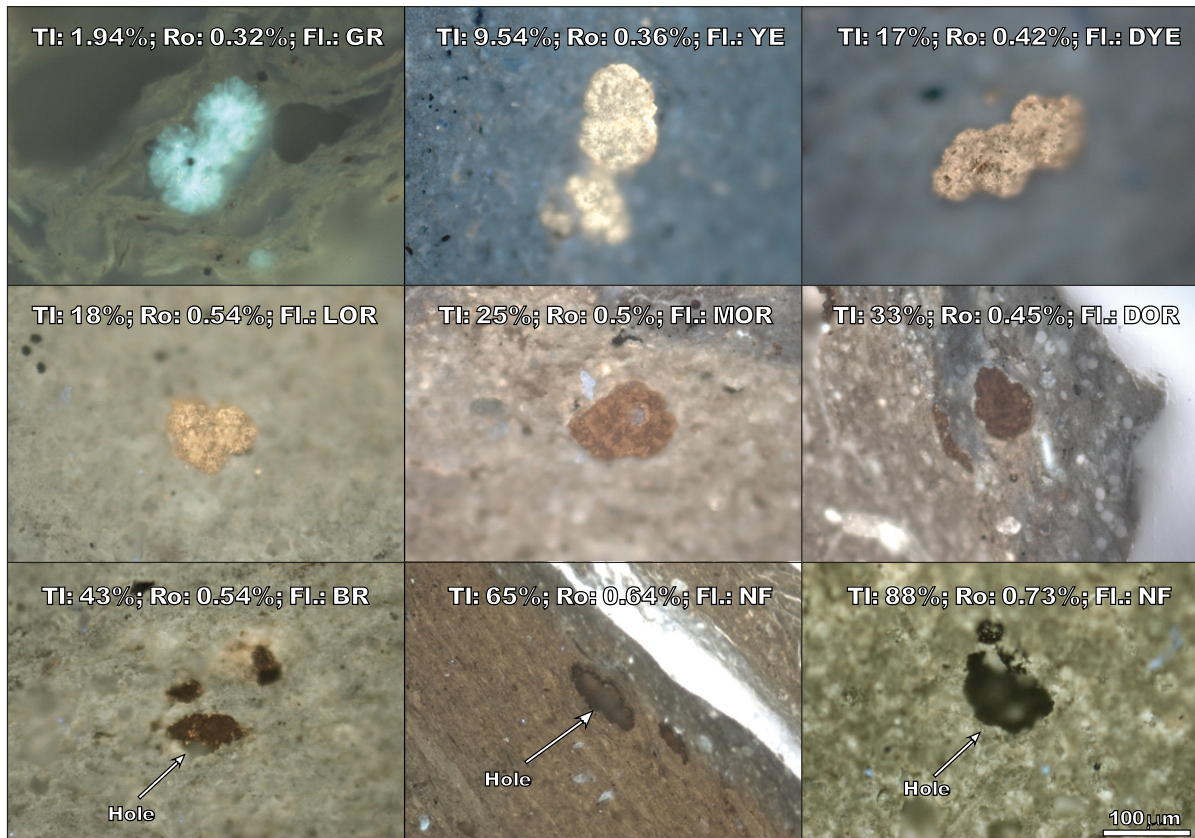


FIGURE I.1. Photomicrographs of fluorescence color of Alginite from the analyzed samples. Legend: Fl. (Fluorescence Color); GR (green); YE (yellow); DYE (dark yellow); LOR (light orange); MOR (middle orange); DOR (dark orange); BR (brown); NF (no fluorescence).

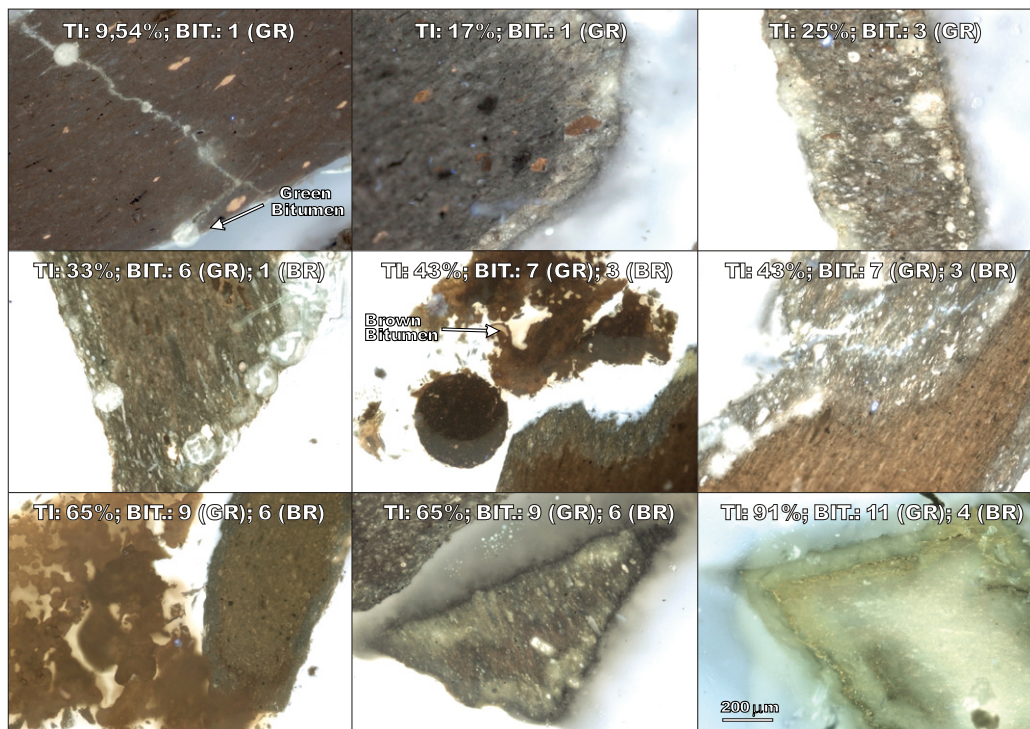


FIGURE I.2. Photomicrographs of bitumens. It is possible to observe two types of bitumen.. Legend: BIT. (Bitumen); GR (green); BR (brown). The number between the parentheses is a semi quantitative scale that was built in order to give a comparative idea between the samples (see Table IV).

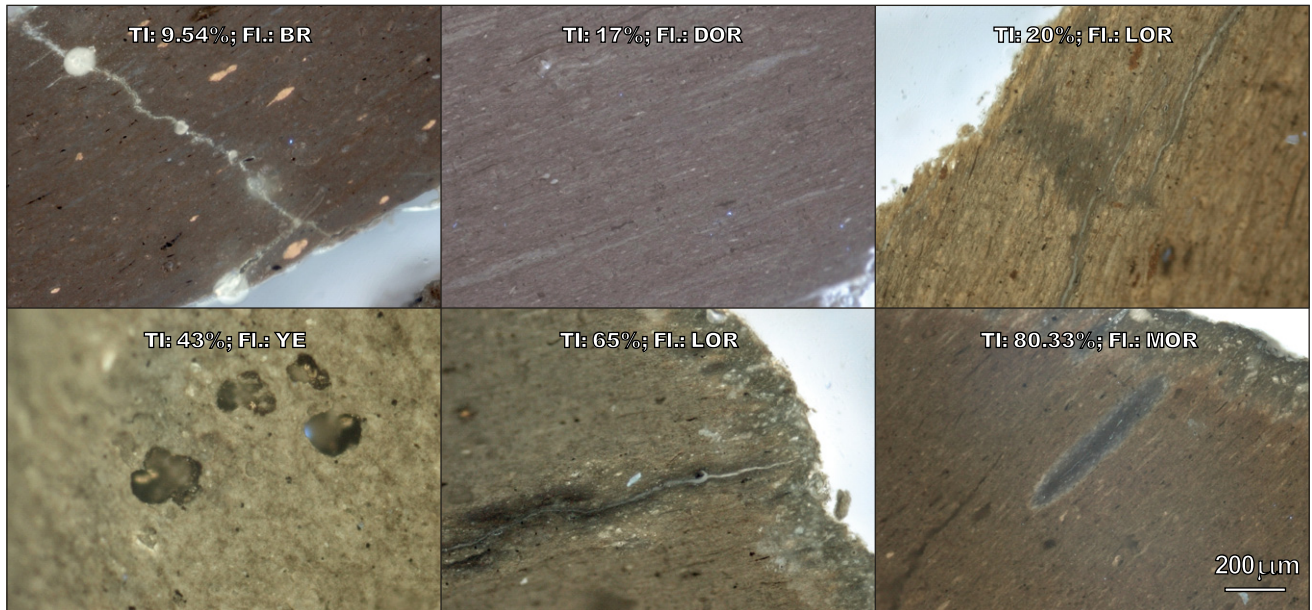


FIGURE I.3. Photomicrographs of fluorescence color of the matrix. Legend: FI. (Fluorescence Color); YE (yellow); LOR (light orange); MOR (middle orange); DOR (dark orange); BR (brown).



FIGURE I.4. Photomicrograph showing different fluorescence color in the matrix of sample with TI of 27.57%. Red arrows are showing the primary migration pathways.

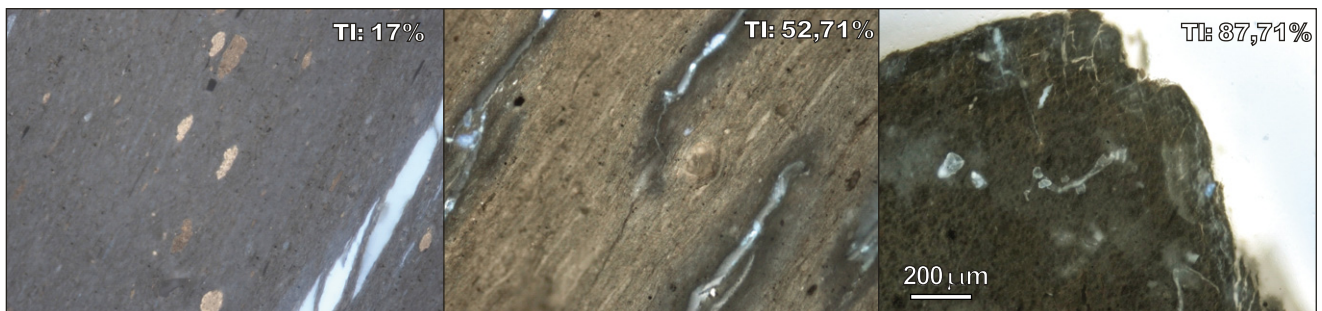


FIGURE I.5. Photomicrographs of fractures.